

**SIMULATION OF THE SYNERGISTIC LOW EARTH ORBIT EFFECTS OF VACUUM  
THERMAL CYCLING, VACUUM UV RADIATION AND ATOMIC OXYGEN**

Joyce A. Dever  
Kim K. de Groh  
NASA Lewis Research Center

Curtis R. Stidham  
Thomas J. Stueber  
Sverdrup Technology, Inc.

Therese M. Dever  
Elvin Rodriguez  
Cleveland State University

Judith A. Terlep  
Case Western Reserve University

**ABSTRACT**

In order to assess the low Earth orbit (LEO) durability of candidate space materials, it is necessary to use ground laboratory facilities which provide LEO environmental effects. A facility combining vacuum thermal cycling and vacuum ultraviolet (VUV) radiation has been designed and constructed at NASA Lewis Research Center for this purpose. This facility can also be operated without the VUV lamps. An additional facility can be used to provide VUV exposure only. By utilizing these facilities, followed by atomic oxygen exposure in an RF plasma asher, the effects of the individual vacuum thermal cycling and VUV environments can be compared to the effect of the combined vacuum thermal cycling/VUV environment on the atomic oxygen durability of materials. The synergistic effects of simulated LEO environmental conditions on materials were evaluated by first exposing materials to vacuum thermal cycling, VUV, and vacuum thermal cycling/VUV environments followed by exposure to atomic oxygen in an RF plasma asher. Candidate space power materials such as atomic oxygen protected polyimides and solar concentrator mirrors were evaluated using these facilities. This paper will discuss characteristics of the Vacuum Thermal Cycling/VUV Exposure Facility which simulates the temperature sequences and solar ultraviolet radiation exposure that would be experienced by a spacecraft surface in LEO. Results of durability evaluations of some candidate space power materials to the simulated LEO environmental conditions will also be discussed. Such results have indicated that for some materials, atomic oxygen durability is affected by previous exposure to thermal cycling and/or VUV exposure.

**INTRODUCTION**

Ground laboratory evaluation of candidate space materials can be used to supplement space flight data for predicting long-term LEO materials durability. Furthermore, because the environmental effects of LEO can act synergistically, it is important to use laboratory facilities which provide combined environmental effects. NASA Lewis Research Center has designed and constructed a facility to provide the combined effects of vacuum thermal cycling and VUV radiation for materials durability evaluation. In this system, heating and cooling are provided through radiative processes in a high vacuum environment. The cycling process simulates space orbital cycles with respect to heating, ultraviolet radiation, and cooling. The heating and ultraviolet radiation exposure occur simultaneously for the

first part of a cycle, then the samples are physically moved to a cooling environment which does not contain VUV. This facility can also be used for vacuum thermal cycling without ultraviolet radiation exposure. The flexible control system developed for this facility permits unattended tests to be safely conducted for long periods of time while preserving the research integrity of the test in the event of any of a variety of malfunctions.

Facilities at NASA Lewis have been used to determine the effects of vacuum thermal cycling (VTC), VUV and combined VTC/VUV on the atomic oxygen durability of materials. Exposure to VTC, VUV and/or combined VTC/VUV is followed by atomic oxygen exposure in an RF plasma asher for such studies. Although the most exhaustive testing would include simultaneous exposure to VTC, VUV and atomic oxygen, facility limitations prevented the inclusion of an atomic oxygen environment with the VTC/VUV combined environment. For this reason, samples are sequentially exposed first to VTC/VUV and then to atomic oxygen. Following this sequence of tests, samples can be analyzed for changes in mass loss rate, optical properties, surface morphology, etc. as compared to samples which were only exposed in the plasma asher. By analyzing results of such testing, it is possible to determine which environmental effects act synergistically on the material being studied. Results have revealed that some materials are synergistically affected by VUV, thermal cycling and atomic oxygen. These results illustrate the importance of utilizing laboratory durability evaluation procedures which permit determination of synergistic effects rather than simply analyzing damage from individual environmental effects.

## SPACE SIMULATION FACILITIES

### Vacuum Thermal Cycling/Vacuum Ultraviolet Radiation Exposure Facility

The VTC/VUV exposure system utilizes a diffusion pumped vacuum system which operates at a pressure of  $< 10^{-6}$  torr. An overall view of the hardware in the VTC/VUV facility is shown in figure 1. Samples are located in the sample holder, as shown, which is physically transported between an environment providing heating and ultraviolet radiation exposure and an environment which allows samples to radiatively cool. Therefore, this facility simulates the thermal cycling and UV exposure to which surfaces in space would be exposed, because heating and UV radiation exposure occur during the sunlit portion of an orbit, and on-orbit cooling occurs in the absence of solar UV radiation when surfaces are in the Earth's shadow. This facility uses two VUV lamps for accelerated VUV exposure in the wavelength range between 115 and 200 nm. A near ultraviolet (NUV) lamp is used to provide UV radiation between 200 and 400 nm; however, because of the long light path from the NUV source to the samples, the NUV intensity is less than one sun. Therefore, the facility is typically referred to as a vacuum thermal cycling/VUV exposure facility, because the shorter wavelength, higher energy VUV, which is most damaging to materials, is accelerated, and the NUV radiation is not accelerated.

#### UV Lamps

As shown in figure 1, two VUV lamps are located inside of the water-cooled shroud. These are 30 watt deuterium lamps with magnesium fluoride windows which provide radiation between 115 and 300 nm; however, the radiation above 200 nm is much less than that of the sun. Therefore these lamps are used for accelerated VUV exposure between 115 and 200 nm. The light path for these lamps is directed upward toward the samples. Also shown is a near ultraviolet (NUV) source which is located outside of the vacuum chamber. This is a 500 watt mercury-xenon short arc lamp which provides radiation of wavelengths between 200 and 400 nm. Light from this source is transmitted through a quartz feedthrough window and directed upward toward the samples using a 90° light bending mirror.

Lamps were individually calibrated using a radiometer/pyroelectric detector system and a series of narrow bandpass filters to obtain irradiance values in air at wavelengths ranging from 180 to 400 nm. Points on a manufacturer-supplied relative spectral irradiance curve (arbitrary units) were multiplied by an appropriate factor, determined from calibration data for the lamp, in order to generate an irradiance curve (in units of power/area x wavelength). Resulting spectral irradiance curves for the combination of VUV and NUV lamps used in this system are shown in figure 2 as compared to the air mass zero solar spectral irradiance. Because VUV wavelengths do not transmit in air, actual VUV irradiance calibrations could not be performed. Therefore, the entire manufacturer-provided VUV lamp irradiance curve between 115 and 300 nm was scaled to fit between the measured data points from 180 to 300 nm. Irradiance curves for the two lamps to be used in the system were summed. Then the integrated intensity between 115 and 200 nm was calculated and used to determine the number of VUV suns. The

ratio of lamp intensity to air mass zero solar intensity in the same wavelength range is referred to as the number of equivalent suns. For the VTC/VUV system, VUV lamps were typically distanced from the sample site such that samples were exposed to approximately 5 VUV suns between 115 and 200 nm. This distance is adjustable for the desired VUV intensity.

Figure 3 shows a plot of the relative intensity (arbitrary units) of a typical VUV lamp as a function of off-axis angle. This data was used to determine the optimum distance between two VUV lamps to minimize the intensity gradient across the 3"x3" sample area.

Because of the long light path to the sample site, the NUV intensity is approximately 0.5 suns. This was calculated by integrating the irradiance curve between 200 and 400 nm. Although 0.5 suns is not an accelerated intensity, the NUV range of wavelengths is represented during exposure.

### Infrared Heating Lamps

The infrared quartz tungsten halogen lamps are also located inside the water-cooled shroud in the VTC/VUV facility as shown in figure 1. These lamps are capable of producing 1000 watts. The actual power to these lamps during the thermal cycling process is controlled using a variable transformer. This is desirable for adjusting the heating rate so that the maximum temperature limit is reached in the same amount of time needed for exposure to a recommended VUV dose.

### Temperature Distribution Across Sample Area in Heating/VUV Environment

Figure 4 shows typical temperature distributions across the sample area for the VTC/VUV system with UV lamps (figure 4a) and without UV lamps (figure 4b). For these experiments, exposed junction thermocouples were located at sites on the sample holder as shown and the lamps were turned on with typical settings and allowed to come to an equilibrium condition. Then readings for the thermocouples were recorded. This experiment was repeated with the NUV and VUV lamps off, because the system is also operated without these lamps. The maximum temperature change between sites was determined to be approximately 22% when operating with the IR, NUV and VUV lamps on and 17% when operating with only the IR lamps. Such temperature variations may result in slightly different levels of damage across a sample surface.

### Cooling Chamber

The liquid nitrogen (LN<sub>2</sub>) cooled copper chamber (see figure 1) provides the surface to which samples radiatively cool during the cooling portion of the cycle. Plumbing for the liquid nitrogen is brazed to the top of the chamber. Insulating composite mica flake sheets were inserted between the bottom of the chamber and the base plate, and "washers" of this same material were used with the mounting screws so that conductive losses to the base plate are minimized.

### Sample Transport Mechanism

The sample holder transport mechanism (see figure 1) provides positioning of the samples between the LN<sub>2</sub> cooled chamber and the heating/VUV exposure section of the facility. The mechanism is a four bar linkage that consists of the drive bar linkage, connecting linkage, swing arm, and the staging platform (ground). Electrical solenoids provide the force input into the system via the drive bar linkage. The drive bar linkage provides the rotation of the connecting linkage which, in turn, drives the swing arm. Test specimens are mounted in a sample holder mounted off the end of the swing arm.

The speed of the transport mechanism is controlled by a variable transformer that provides electrical power to the solenoids. The linkage system is designed such that sudden changes in acceleration (jerk) and deceleration are minimized on the samples as they are moved between the heating/VUV and cooling positions, and mechanical advantage is maximized when needed. The angle between the connecting linkage and the swing arm is 45 degrees when the samples are both in the cooled chamber and the VUV exposure/heating section. This angle results in an initial slip at the pin-slot interface when the solenoids are energized. The linkage design, along with controlled minimal power to the solenoids, results in a smooth transport of the test samples in the cycle process.

## Thermocouple Temperature Monitors

To provide the most realistic temperature response for the particular material being tested, exposed junction thermocouples are attached to a surface or embedded in a film material simulating the material being thermal cycled. A thermocouple is used to obtain a strip chart readout of the temperature as a function of test time. Thermocouples can also be utilized for controlling the thermal cycling process as described in the following section.

## VTC/VUV Control System

A programmable logic controller (PLC) is utilized for monitoring and controlling the VTC/VUV process permitting safe operation for long-term unattended tests. The controller actuates the solenoids of the sample transport mechanism to move a sample from the heated/VUV environment to the cooling chamber and then returns the samples to the heated/VUV environment to complete the cycle. With the PLC, the user can select from three methods of VTC/VUV control: manual control, temperature control or timer control.

Using manual control, the operator observes the temperature on a thermocouple readout, and, when the desired temperature is reached, actuates the sample transporter to move between the heating/VUV and cooling environments.

With temperature control, the PLC monitors the temperature from a thermocouple and automatically moves the samples between the heating/VUV and cooling environments at the appropriate temperature limits. Two thermocouples are monitored by individual meter/relays with dual manually adjustable set points. These meter/relays monitor and display sample temperature. One of these signals the controller to move the samples between environments at the appropriate programmed temperatures. The other is programmed with set-points slightly beyond the thermal cycling temperature limits. In the event that its temperature limits are exceeded due to failure of a solenoid or failure of the first thermocouple, this meter/relay signals the PLC. If this occurs, the test is automatically discontinued, and an error indicator is energized. The number of completed cycles is saved in the PLC memory, and samples remain under vacuum.

Using timer control, the operator can program the PLC to expose samples in each environment for predetermined amounts of time. Due to the flexibility of the control system and the repeatable nature of the thermal cycling process, the user can operate the system manually to determine the amount of time needed in each of the heating/VUV and cooling environments, program the PLC with these time durations, and complete the test using timer control. This is the method typically used, because of its convenience in only using one thermocouple, for the chart recorder, and because it is reliable.

For the most precise control of the sample cycling temperatures without concern for sample overheating, the system can be operated in temperature limit mode coupled with timer mode. Using this method of operation, the timer mode takes over for the remainder of the test in the event of thermocouple system failure.

At any time during the process, the user has the option of manually moving a sample between environments or terminating the test. The user defines the end of the test by programming the PLC with the number of cycles required. The user can display the number of cycles completed on the PLC readout.

The PLC also monitors the cooling chamber temperature, water-cooled shroud temperature, VUV, NUV and IR lamp status (on or off), bell jar vacuum, cooling water flow switches and solenoid movement. Malfunctions result in process shutdown, energizing of the appropriate indicator light for the malfunction, and maintenance of vacuum (if possible) until the user can correct the condition.

## **Vacuum Ultraviolet Radiation Exposure Facility**

The VUV Exposure Facility contains three water cooled copper compartments each equipped with a 30 watt deuterium lamp with a magnesium fluoride window. These compartments are located inside of a diffusion pumped high vacuum system bell jar which operates at a pressure of approximately  $2 \times 10^{-6}$  torr. Samples are located on the floor of these compartments. The stainless steel base plate of each compartment is instrumented with a thermocouple. The distance between the lamp and the sample was adjusted for the desired VUV intensity.

## **RF Plasma Asher**

The atomic oxygen environment of LEO was simulated using an RF plasma asher which generates a 13.56 Mhz RF discharge of oxygen or air, depending on which feed gas is used. Samples were placed on a glass rack in the

center of the asher which can support a sample area of approximately 3 inches by 6 inches. Various species of oxygen (and nitrogen, if air is the feed gas) atoms, ions and molecules are contained in the plasma. This discharge results in random directional thermal energy atomic oxygen attack of samples. It is expected that the only reactive species are the oxygen species, because nitrogen species were not found to contribute to the erosion of a polyimide material [1]. Samples located in the plasma are also exposed to a high intensity of VUV radiation at the 130 nm oxygen resonance line [2]. Intense spectral lines from nitrogen species also occur in the VUV [3], and are present in the plasma when an air is used as a feed gas.

## DURABILITY EVALUATIONS USING SIMULATED SPACE ENVIRONMENTS

A variety of materials have been analyzed for their changes in atomic oxygen durability due to previous exposure to VTC, VUV and/or combined VTC/VUV. Experimental procedures and results of these studies are described in the following sections.

### Candidate Atomic Oxygen Protective Solar Array Blanket Materials

Solar array blankets are intended to provide structural support and the proper thermal environment for efficient performance of the Space Station Freedom Photovoltaic Power System. Candidate materials have been analyzed for their durability and performance upon exposure to simulated LEO environments. These candidate materials have included  $\text{SiO}_x$  (where  $x$  is approximately 2) coated Kapton<sup>®</sup> film (Kapton is a registered trademark of DuPont), manufactured by Sheldahl, and polysiloxane-polyimide film made from silicone and polyimide cast from a solution mixture which were manufactured by DuPont. Two types of this polysiloxane-polyimide material, 93-1 and AOR Kapton, were studied. The 93-1 is an earlier formulation of the AOR Kapton material. The polysiloxane-polyimide materials are atomic oxygen protective, because silicone surfaces are expected to form a skin of  $\text{SiO}_x$  upon exposure to atomic oxygen [4], and  $\text{SiO}_x$  has been found to be an effective barrier to atomic oxygen attack [1, 4-6].

Solar array blanket surfaces are expected to see temperature swings between  $+80^\circ\text{C}$  and  $-80^\circ\text{C}$  in Space Station Freedom orbit. During each orbit, surfaces will be exposed to sunlight for approximately 59 minutes. These specifications were used for materials testing in the VTC/VUV facility. The VUV lamps were arranged to provide 5 VUV suns, so the time needed for samples to receive the same amount of VUV that they would receive in an orbit was 11.8 minutes (59 minutes/5 suns). The heating rate was adjusted so that the temperature change from  $-80^\circ\text{C}$  to  $+80^\circ\text{C}$  was accomplished in the same amount of time. It is important to note that different materials will have different thresholds of ultraviolet intensity which can be tolerated and above which unrealistic damage will occur. Results of accelerated VUV exposure must, therefore, be interpreted with caution unless a comparison can be made between damage at a level of one sun and at the level desired to be used. If a material passes a highly accelerated test, then it is probable that it will survive in the real-time space environmental exposure. However, a material which fails due to overtesting may still perform well in the space environment. For this reason, accelerated tests yield very conservative results.

#### DuPont 93-1 and AOR Kapton

Figure 5 shows the fractional mass loss of samples of 93-1 upon exposure to the atomic oxygen environment of an RF air plasma asher [7]. The sample previously exposed to 1000 ESH VUV showed a fractional mass loss of approximately 1.5 times that of the sample not previously exposed; however, the data may be within experimental error of each other. The sample exposed to VTC/VUV showed a fractional mass loss per unit area of approximately 2 times that of the sample not previously exposed. Furthermore, the data does not appear to be within experimental error of the data from samples not exposed to VUV prior to atomic oxygen exposure. Figure 6 shows scanning electron micrographs of a sample which was only plasma ashed and a sample which was plasma ashed following VTC/VUV exposure. Note that the sample which was only ashed (figure 6a) showed undercutting due to atomic oxygen erosion primarily at linear defect areas on the sample. These linear defect areas were probably produced during processing of this material. The sample exposed to 700 VTC/VUV cycles then air plasma ashed (figure 6b) showed a significantly different type of atomic oxygen damage than the previously unexposed sample. Note the severe branching of cracks with atomic oxygen undercutting. It is possible that the VTC/VUV exposure resulted in cracking at the silicone enriched surface of the film which became visible as atomic oxygen undercutting took place.

As shown in figure 7 [8], exposure to VTC/VUV had a reversed effect on the AOR Kapton material as

compared to its effect on the 93-1 material. In fact, previous exposure to VUV or VTC/VUV resulted in significantly improved atomic oxygen resistance for AOR. The surface of the AOR Kapton material appeared to have "water spots" possibly due to a release agent used in the processing of the material which left a residue on the surface. This residue was not observed on the 93-1 material. This residue may affect the VTC, VUV and/or atomic oxygen reactions with the material. Other undisclosed processing changes between 93-1 and AOR Kapton may also have affected the materials' durability to these environmental effects which would explain the different behavior for these two materials.

### SiO<sub>x</sub> Coated Kapton

Figure 8 [8] shows that there is little difference in the atomic oxygen susceptibilities of samples of pristine, VUV exposed and VTC/VUV exposed SiO<sub>x</sub>/Kapton. Although these samples were exposed to a fraction of the fluence that the 93-1 and AOR Kapton samples received, the trends in atomic oxygen degradation are obvious.

## **Solar Concentrator Mirror Materials**

### Candidate Space Station Freedom Solar Concentrator Materials

Solar concentrator coupons were composed of a sandwich type structure of two sheets of graphite epoxy bonded to an aluminum honeycomb core. Coupons of this type were fabricated at Hercules Aerospace and sent to 3M Corporation where copper (an adhesion promoting layer), silver (a reflecting layer), aluminum oxide and silicon dioxide (atomic oxygen protective layers) were deposited onto the face sheets of the coupons. These samples were exposed to VUV and to VTC/VUV followed by atomic oxygen exposure [9]. Coupons were exposed to thermal cycling between -17.8°C and +121°C, and a VUV intensity of 5 VUV suns was used. The heating rate was adjusted so that the temperature change from the minimum to the maximum temperature was accomplished in the amount of time necessary for exposure to a full orbital VUV dose, 11.8 minutes, equivalent to 59 minutes of exposure to sunlight in LEO. Figure 9a shows changes in spectral specular reflectance for a coupon exposed first to 1000 ESH VUV at an intensity of 3 equivalent suns, then to an atomic oxygen fluence of  $1.4 \times 10^{21}$  atoms/cm<sup>2</sup>. Exposure to VUV caused a significant decrease in the specular reflectance centered at a wavelength of approximately 375 nm, and the sample showed a yellow discoloration. This may be due to either VUV induced color center formation, referred to as solarization, in the SiO<sub>2</sub> and/or Al<sub>2</sub>O<sub>3</sub> layers or to a layer of contamination which may have settled on the surface due to volatilization of organics from adhesives upon heating by the VUV lamps. Subsequent exposure to atomic oxygen resulted in reversal of this damage which is thought to be due to either "bleaching," oxidation resulting in reversal of the chemical reactions which occurred upon VUV exposure, or a thermal effect due to heating of metals in the plasma asher. Solarization has been known to reverse in some cases with heat treatment [10]. Metals are known to heat up during plasma asher exposure as evidenced by an aluminum sample instrumented with a temperature strip which reached a temperature of approximately 104°C during exposure.

The sample exposed to 908 vacuum thermal cycles containing 893 ESH VUV experienced the same type of spectral changes in specular reflectance as the VUV exposed sample. However, the extent of this damage was less as shown in figure 9b. This may be due to a competition between VUV induced degradation and thermal "annealing" of this damage. As with the VUV exposed sample, the VTC/VUV damage is somewhat reversed by subsequent exposure to atomic oxygen.

Possible conclusions from this data are that VUV damage and atomic oxygen bleaching are competing processes which may occur upon exposure to these two environments simultaneously. If bleaching of color centers is the mechanism of atomic oxygen reaction with this coupon, then the damage observed due to VUV radiation alone may be more severe than the on-orbit behavior of a solar concentrator mirror, because atomic oxygen may be able to reverse this damage. Another possible conclusion is that heat treatment results in the reversal of the VUV damage. It is likely that this was the reason that the VTC/VUV exposed sample was less damaged than the VUV exposed sample. Furthermore, if extensive heating occurred upon plasma asher exposure, this may explain the reversal of damage for both samples. As mentioned previously, it is important to interpret results of accelerated testing with caution. It is not known whether the severity of damage would have been the same for samples exposed to less VUV intensity for the same number of equivalent sun hours. Therefore, it is expected that the results of this testing are conservative and are not likely to be representative of real-time exposure but, rather, they represent worst-case degradation.

## Sol-gel Planarized Mirrors

Sol-gel planarized mirrors, developed by Sandia National Laboratories, have been considered for advanced solar concentrator applications. The sol-gel mirrors described in this study consisted of a stainless steel foil substrate, a silicate sol smoothing layer, a silver reflecting layer, a silicon oxide layer and finally a silicate sol atomic oxygen protective layer. The surface layer on Sample A consisted of a silicate sol with a hydrolysis ratio of 1:10. Sample B contained a surface layer of silicate sol with a hydrolysis ratio of 1:5. These samples were incrementally atomic oxygen exposed in the plasma asher followed by exposure to vacuum thermal cycling between  $-18^{\circ}\text{C}$  and  $+93^{\circ}\text{C}$  without VUV exposure. Changes in solar specular reflectance of these samples as a function of atomic oxygen exposure and vacuum thermal cycling are shown in figure 10a-b. Sample A displayed a significant decrease in solar specular reflectance upon exposure to an atomic oxygen fluence of  $1.3 \times 10^{21}$  atoms/cm<sup>2</sup>. An air plasma ashed sample of exactly the same composition was analyzed using Auger Electron Spectroscopy and showed evidence of Ag and Fe in the silicate sol top layer. This may be due to thermally induced diffusion of silver and iron from underlying layers due to heating which accompanies plasma ashing and may be responsible for the reduced solar specular reflectance. Sample B, in contrast, showed a slight improvement in solar specular reflectance upon exposure to the same atomic oxygen fluence; however, this may have been within experimental error, because the exposed samples showed variations in appearance across their surface, and it was difficult to measure the sample in exactly the same location each time, it is expected that there was some error associated with each of these reflectance measurements. Both samples showed significant decreases in reflectance upon subsequent exposure to 10 vacuum thermal cycles. It is likely that heating during the thermal cycling resulted in further diffusion of metal species from underlying layers resulting in this specular decrease. Continued exposure to both ashing and thermal cycling led to smaller changes in specular reflectance for both samples. From this data, it is difficult to determine how, if at all, atomic oxygen affected these samples. However, because the temperature suspected in the asher,  $104^{\circ}\text{C}$ , was only slightly higher than the maximum temperature during thermal cycling,  $93^{\circ}\text{C}$ , it is likely that this thermally induced diffusion effect would occur on surfaces of this type exposed in space. Other information, such as combined effects of vacuum thermal cycling and VUV would be necessary in conducting a thorough LEO durability and performance evaluation of this material.

## **CONCLUDING REMARKS**

It is important to utilize ground laboratory facilities and procedures which provide the synergistic effects likely to occur in the LEO environment when conducting durability and performance evaluation of candidate space materials. Data obtained from exposure of materials to a combined environment containing both vacuum thermal cycling and VUV radiation followed by atomic oxygen exposure can be compared to data from exposure to the singular environments of VUV or vacuum thermal cycling prior to ashing. This type of test matrix can be used to determine whether these environments are expected to react synergistically with the material being tested. The VTC/VUV exposure facility designed and constructed at NASA Lewis provides the capability of evaluation of the synergistic effects of vacuum thermal cycling and VUV radiation and, along with other NASA Lewis facilities, can be used in such a test matrix. Candidate materials for use on space power system surfaces have been evaluated utilizing these facilities to determine potential LEO synergistic effects. Results indicated that for some materials, such as the solar concentrator mirrors, there is a competitive process between VUV or VTC/VUV induced damage and atomic oxygen reversal of this effect. This type of behavior should be considered when predicting the in-space performance of a concentrator mirror. For materials such as DuPont 93-1, cracking due to VTC/VUV exposure may result in degradation of the material which would not have been observed upon exposure to atomic oxygen alone. In the case of AOR Kapton, VUV and VTC/VUV exposure resulted in improved atomic oxygen durability. Materials such as the sol-gel mirrors appear to be sensitive to heating and it is unknown what affect, if any, atomic oxygen has on these surfaces.

Data from the tests summarized above show the wide range of synergistic reactions possible between vacuum thermal cycling, VUV and atomic oxygen on various types of materials and illustrate the importance of evaluating these synergistic effects when conducting durability and performance testing. Finally, caution must be used when interpreting the results of accelerated testing, because materials which fail due to overtesting may still adequately survive real-time space exposure.

## REFERENCES

1. Rutledge, S. K. et al.: "An Evaluation of Candidate Oxidation Resistant Materials for Space Applications in LEO." NASA Technical Memorandum No. 100122. Paper presented at the Workshop on Atomic Oxygen Effects, Pasadena, CA. 1986.
2. Koontz, S. L.; Albyn, K; and Leger, L. J.: "Atomic Oxygen Testing with Thermal Atom System: A Critical Evaluation." Journal of Spacecraft and Rockets. Vol. 28, No. 3, May-June 1991, pp. 315-323.
3. Zaidel, A. N.; and Shreider, E. Ya.: Vacuum Ultraviolet Spectroscopy. Ann Arbor-Humphrey Science Publishers, Ann Arbor, MI, 1970, p. 195.
4. Rutledge, S. K.; and Mihelcic, J. A.: "The Effect of Atomic Oxygen on Altered and Coated Kapton Surfaces for Spacecraft Applications in Low Earth Orbit." Materials Degradation in Low Earth Orbit, V. Srinivasin and B. A. Banks, eds. The Minerals, Metals and Materials Society, 1990, pp. 35-48.
5. Banks, B. A. et al.: "Ion Beam Sputter-Deposited Thin Film Coatings for Protection of Spacecraft Polymers in Low Earth Orbit." NASA Technical Memorandum No. 87051, January 1985.
6. Banks, B. A. et al.: "Sputtered Coatings for Protection of Spacecraft Polymers." NASA Technical Memorandum 83706, April 1984.
7. Brady, J. A. and Banks, B. A.: "Vacuum Ultraviolet and Thermal Cycling Effects on Atomic Oxygen Protective Photovoltaic Array Blanket Materials." Materials Degradation in Low Earth Orbit, V. Srinivasin and B. A. Banks, eds. The Minerals, Metals and Materials Society, 1990, pp. 133-43.
8. Dever, J. A.; Bruckner, E. J. and Rodriguez, E.: "Synergistic Effects of Ultraviolet Radiation, Thermal Cycling and Atomic Oxygen on Altered and Coated Kapton Surfaces." American Institute of Aeronautics and Astronautics. Paper No. 992-0794. Presented at the AIAA 30th Aerospace Sciences Meeting and Exhibit, Reno, NV, January 1992.
9. de Groh, K. K. et al.: "Low Earth Orbit Durability Evaluation of Solar Concentrator Materials." Solar Engineering 1992, Vol. 2, William Stine et al., eds., The American Society of Mechanical Engineers, 1992.
10. Koller, L. R.: Ultraviolet Radiation. John Wiley & Sons, Inc., N.Y. 1965, p. 169.

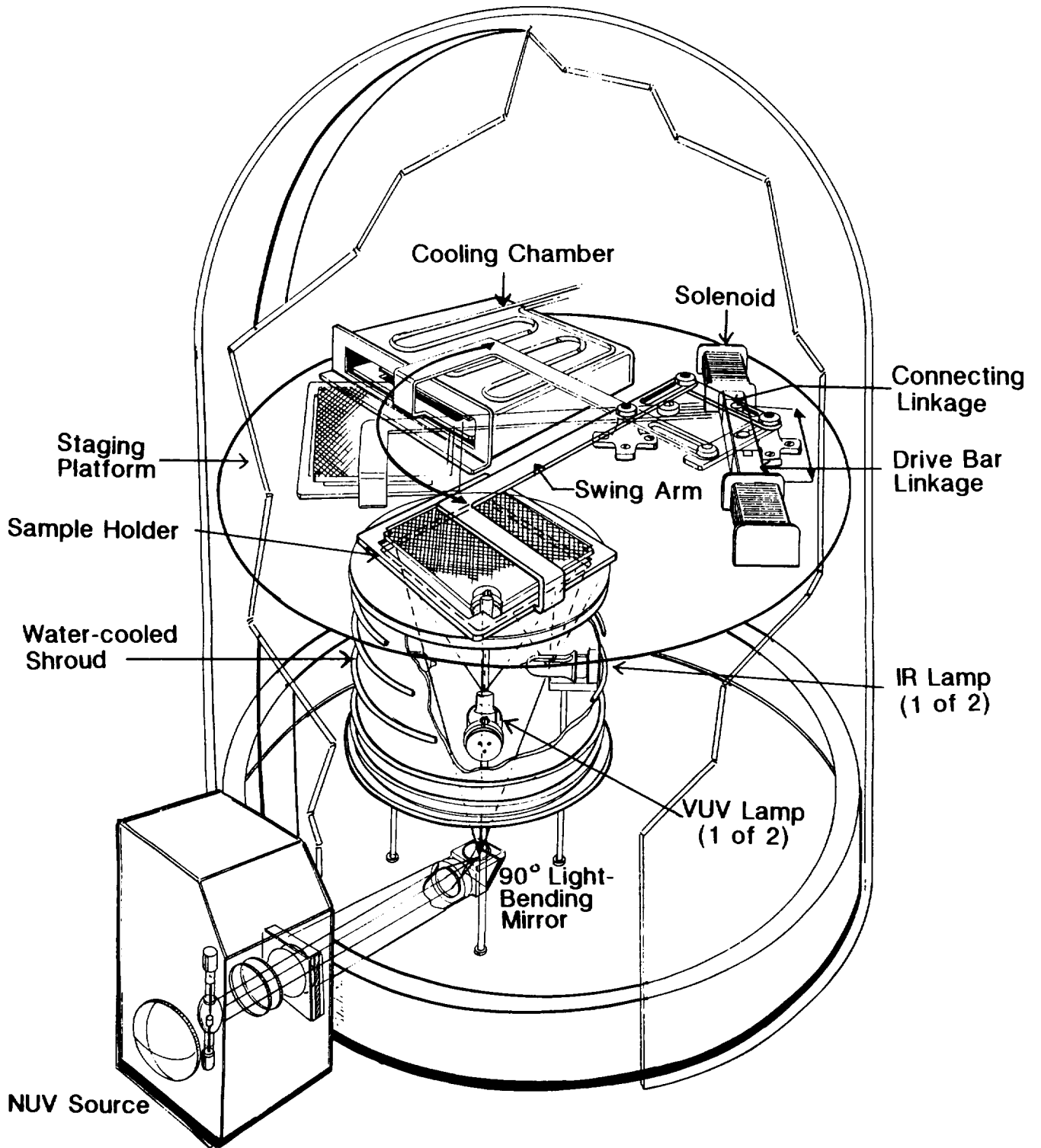


Figure 1: Vacuum Thermal Cycling/VUV Exposure System.

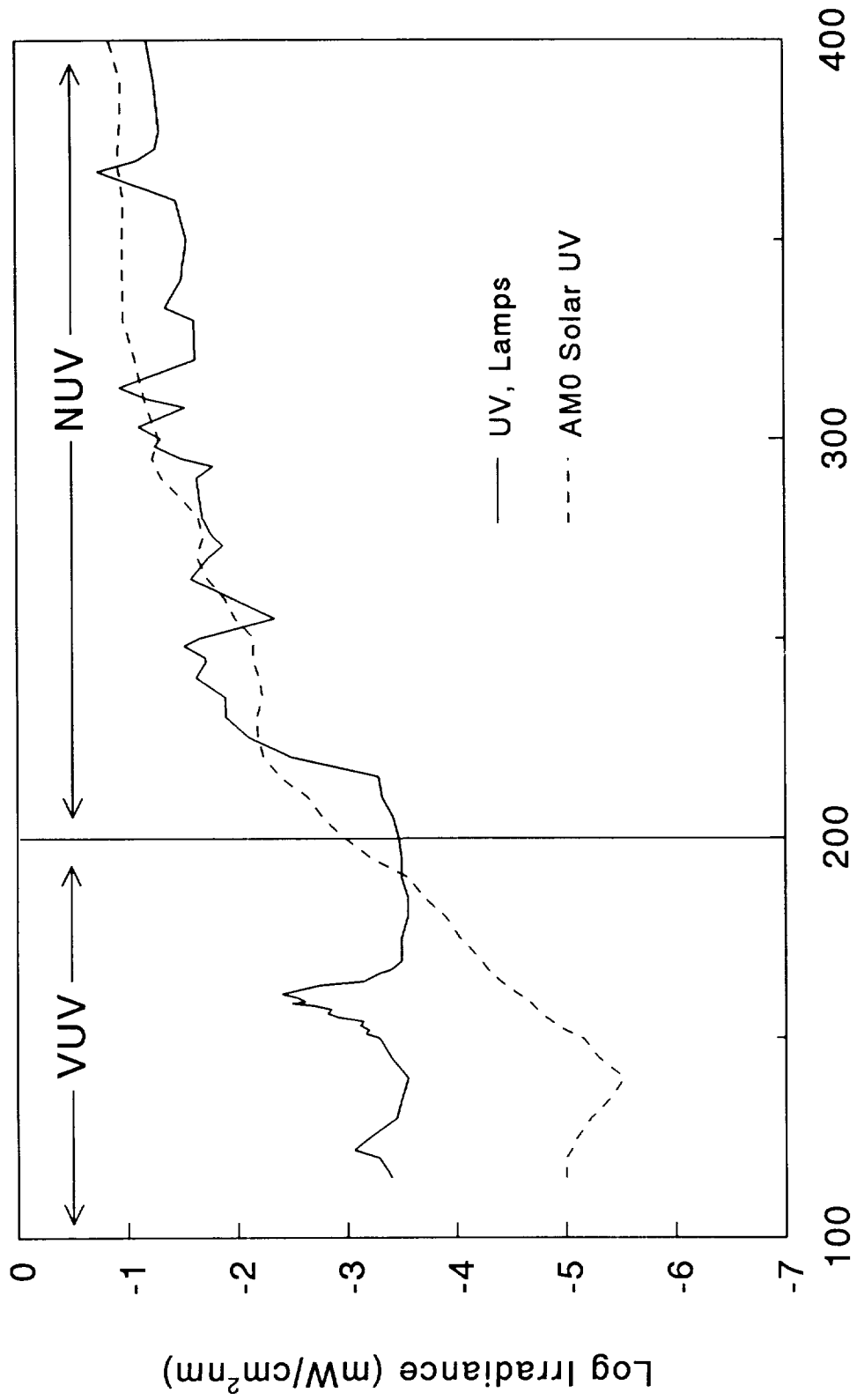
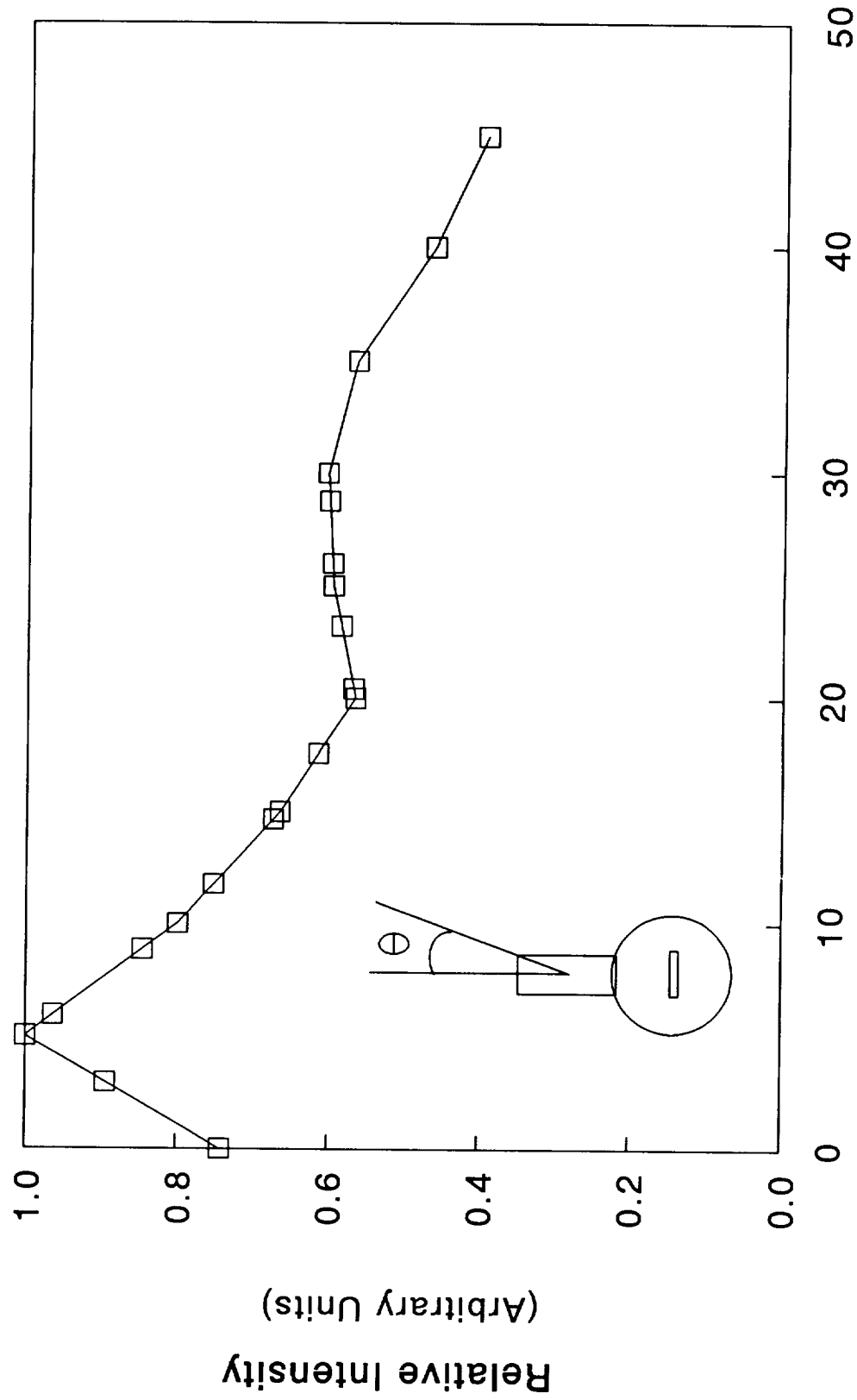
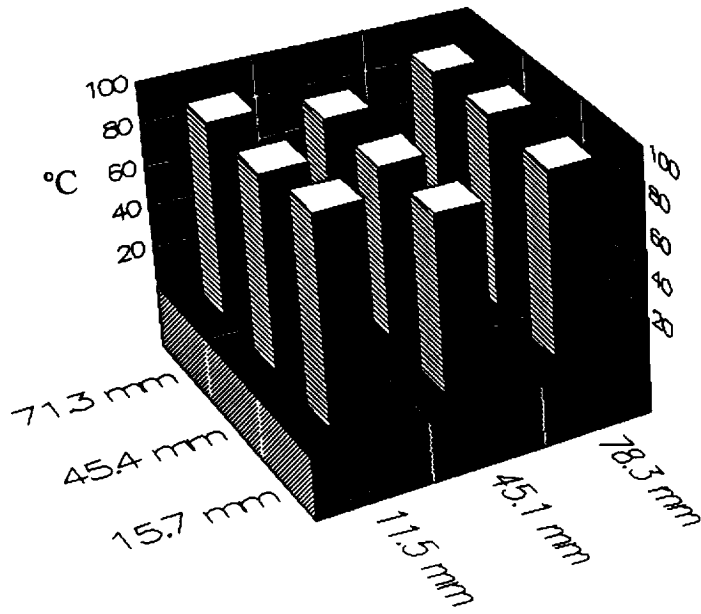


Figure 2: Spectral irradiance measured in air for VUV and NUV lamps used in VTC/VUV system as compared to air mass zero solar irradiance.

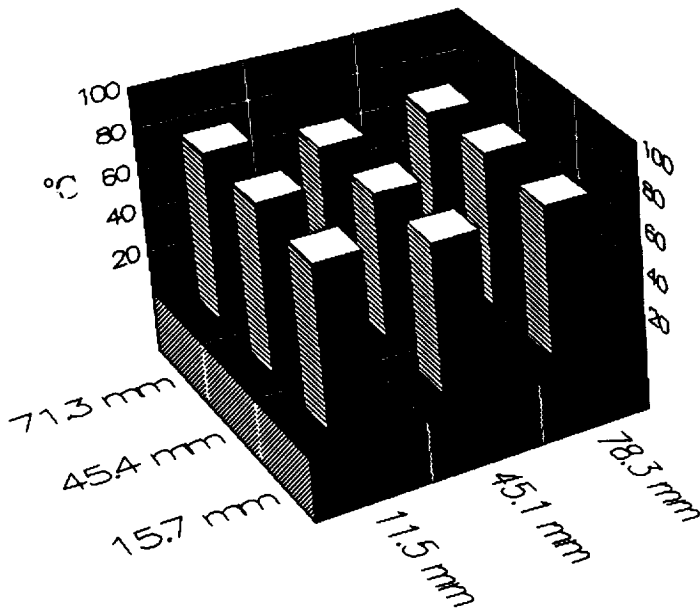


**Off-Axis Angle  $\Theta$ , degrees**

**Figure 3:** Relative intensity of a typical VUV lamp as a function of off-axis angle.



**a**



**b**

**Figure 4:** Typical temperature distributions across VTC/VUV system sample holder a) using VUV, NUV and IR lamps, and b) using only IR lamps.

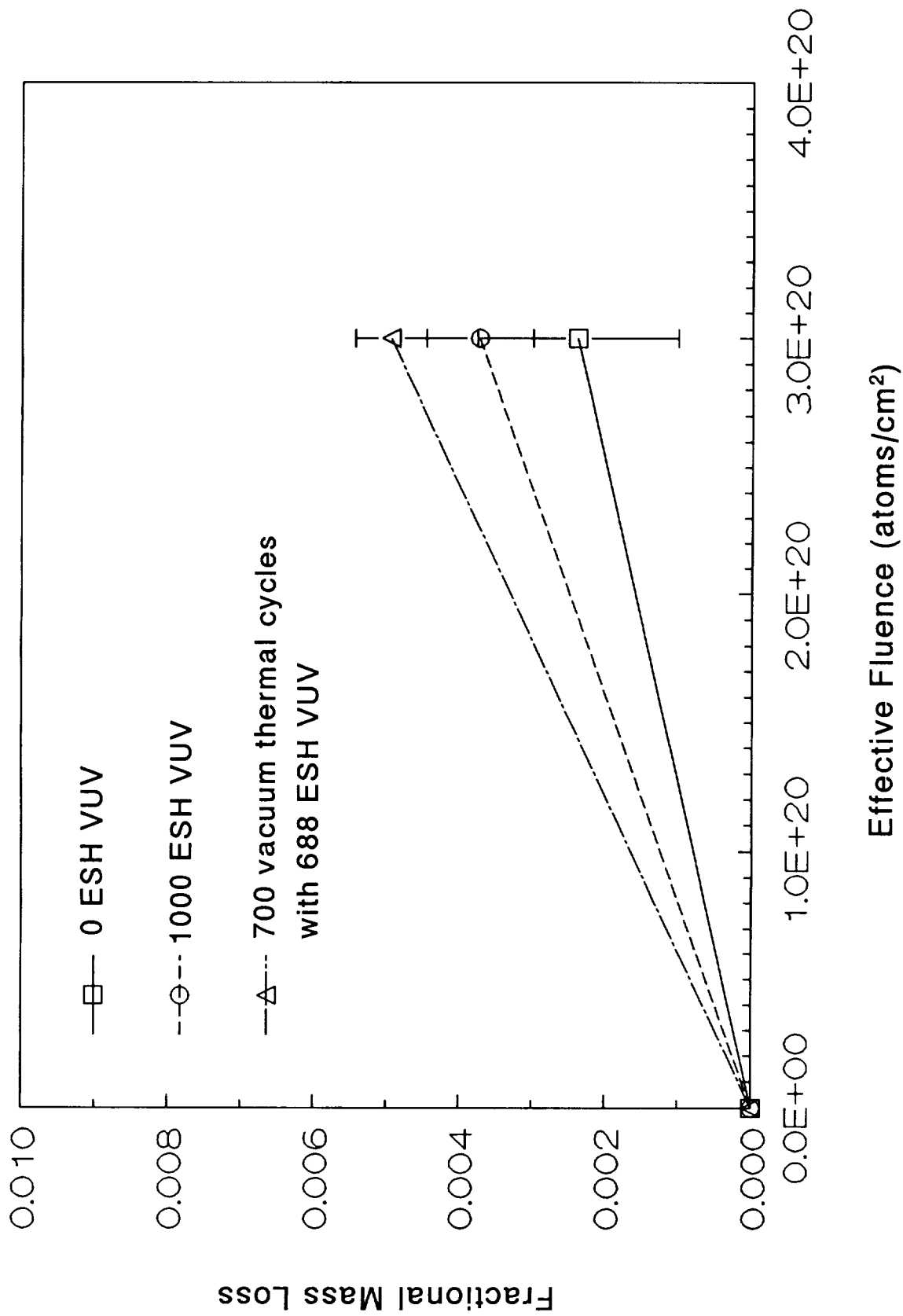


Figure 5: Atomic oxygen erosion of DuPont 93-1 exposed in a plasma asher.

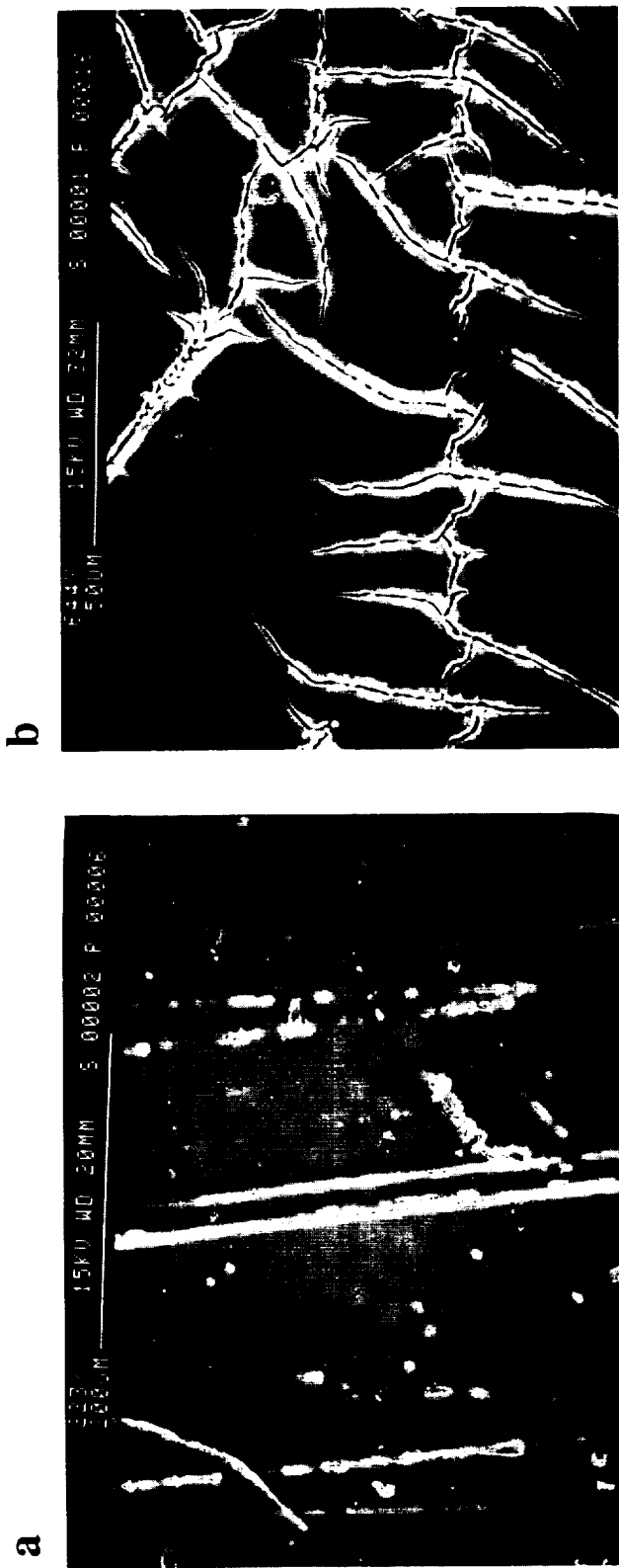


Figure 6: SEM photographs of DuPont 93-1 exposed to a) atomic oxygen (effective fluence =  $3 \times 10^{20}$  atoms/cm<sup>2</sup>) and b) 700 vacuum thermal cycles with 688 ESH VUV followed by exposure to atomic oxygen (effective fluence =  $3 \times 10^{20}$  atoms/cm<sup>2</sup>).

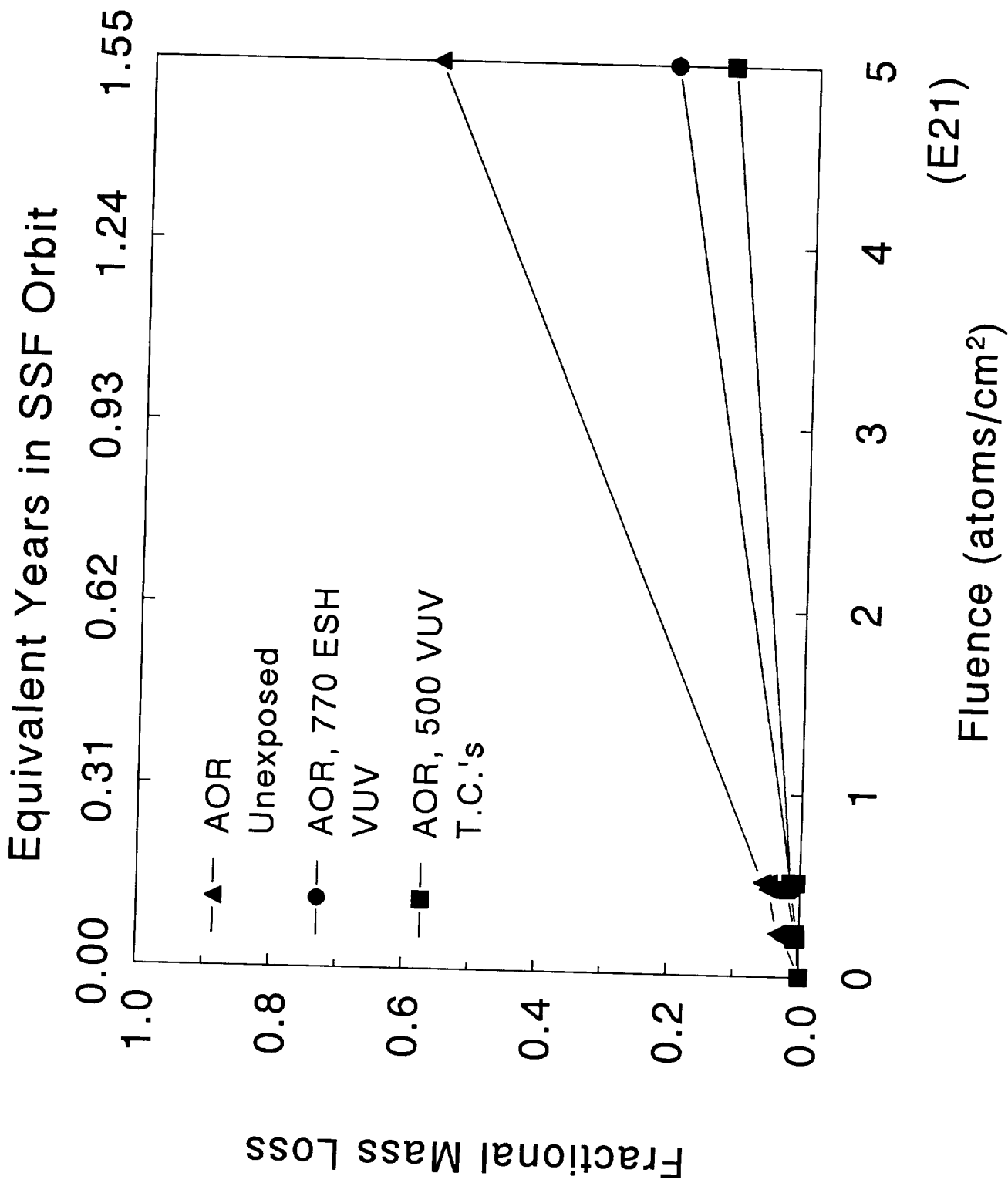


Figure 7: Atomic oxygen erosion of AOR Krypton exposed in a plasma asher.

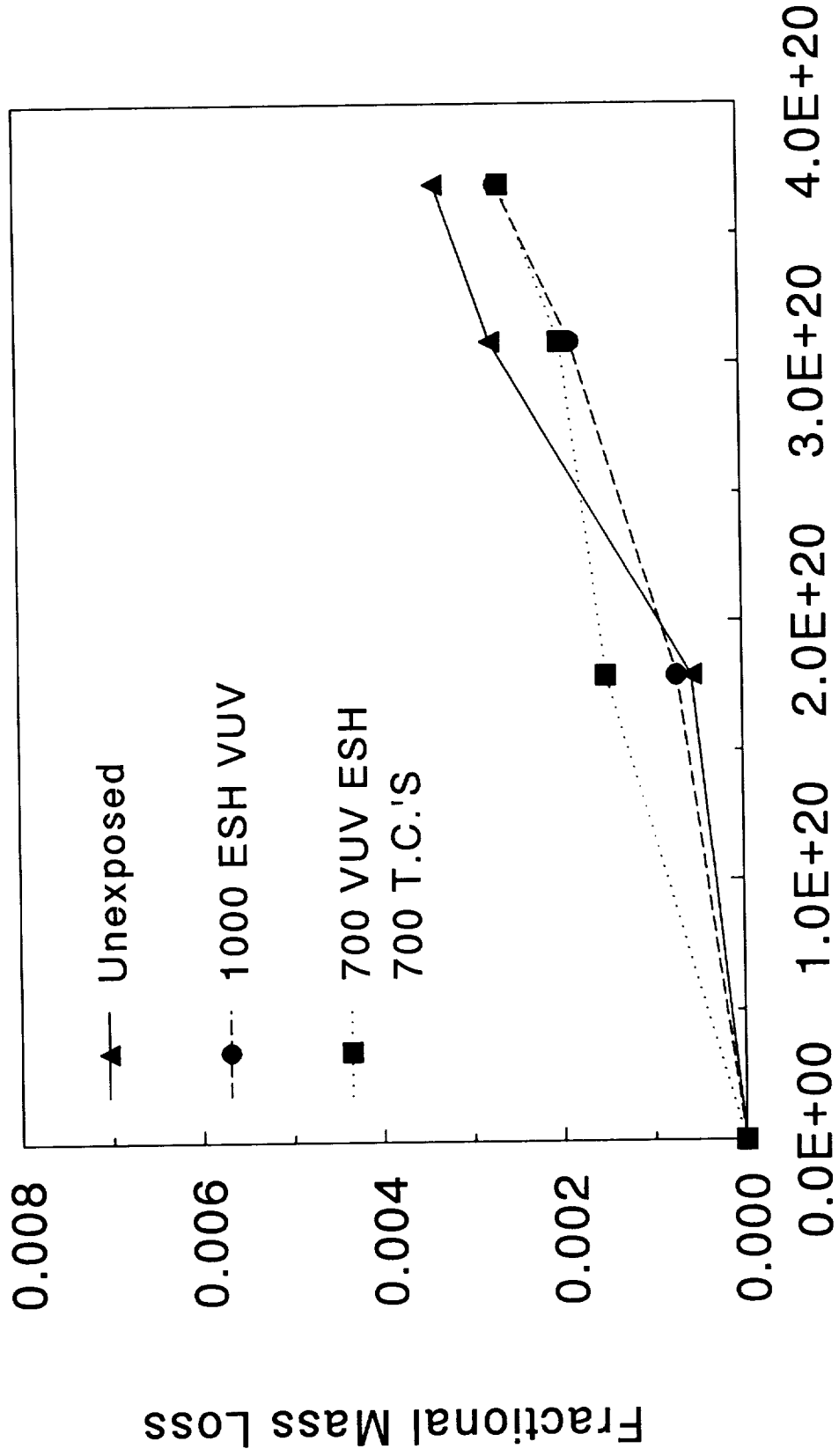


Figure 8: Atomic oxygen erosion of SiO<sub>x</sub> coated Kapton exposed in a plasma asher.

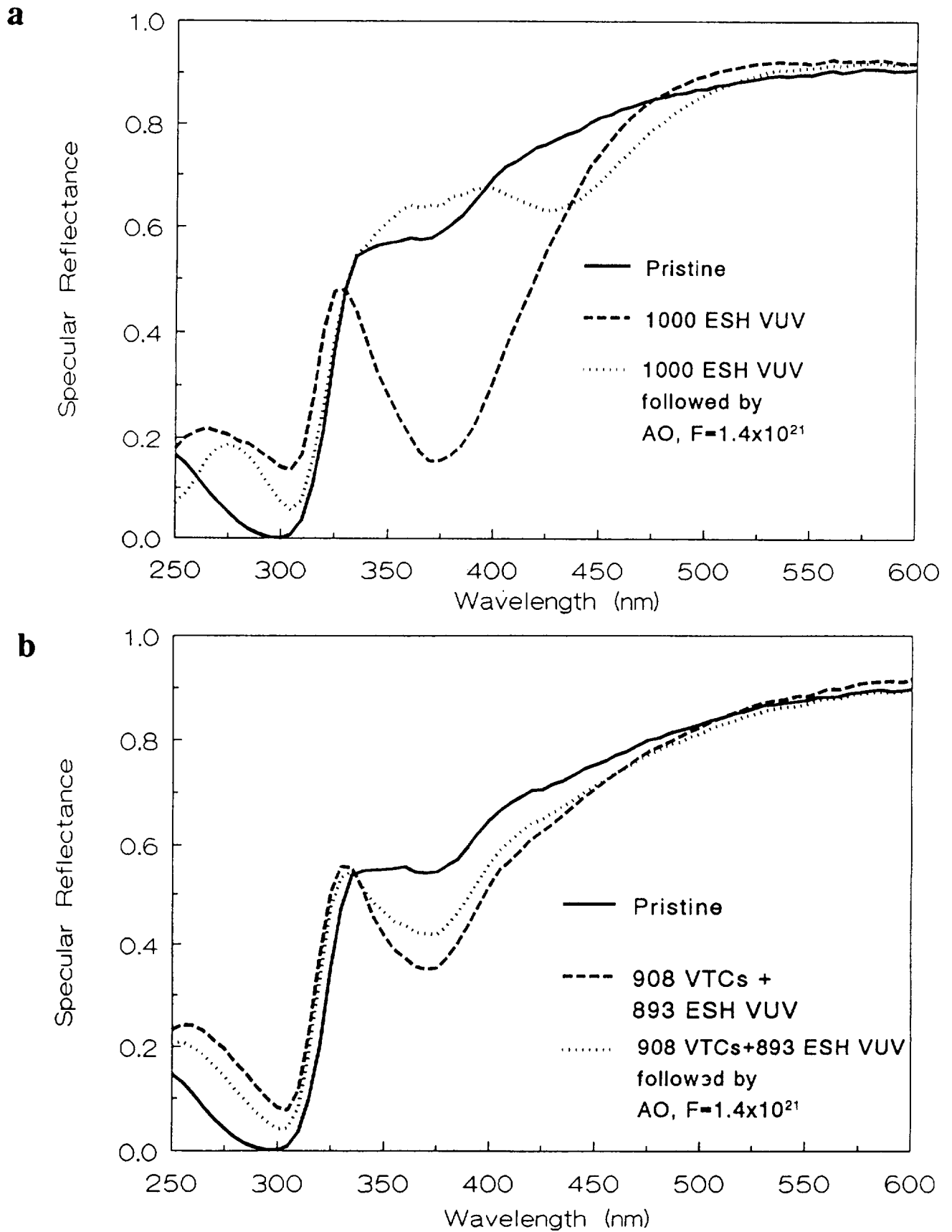
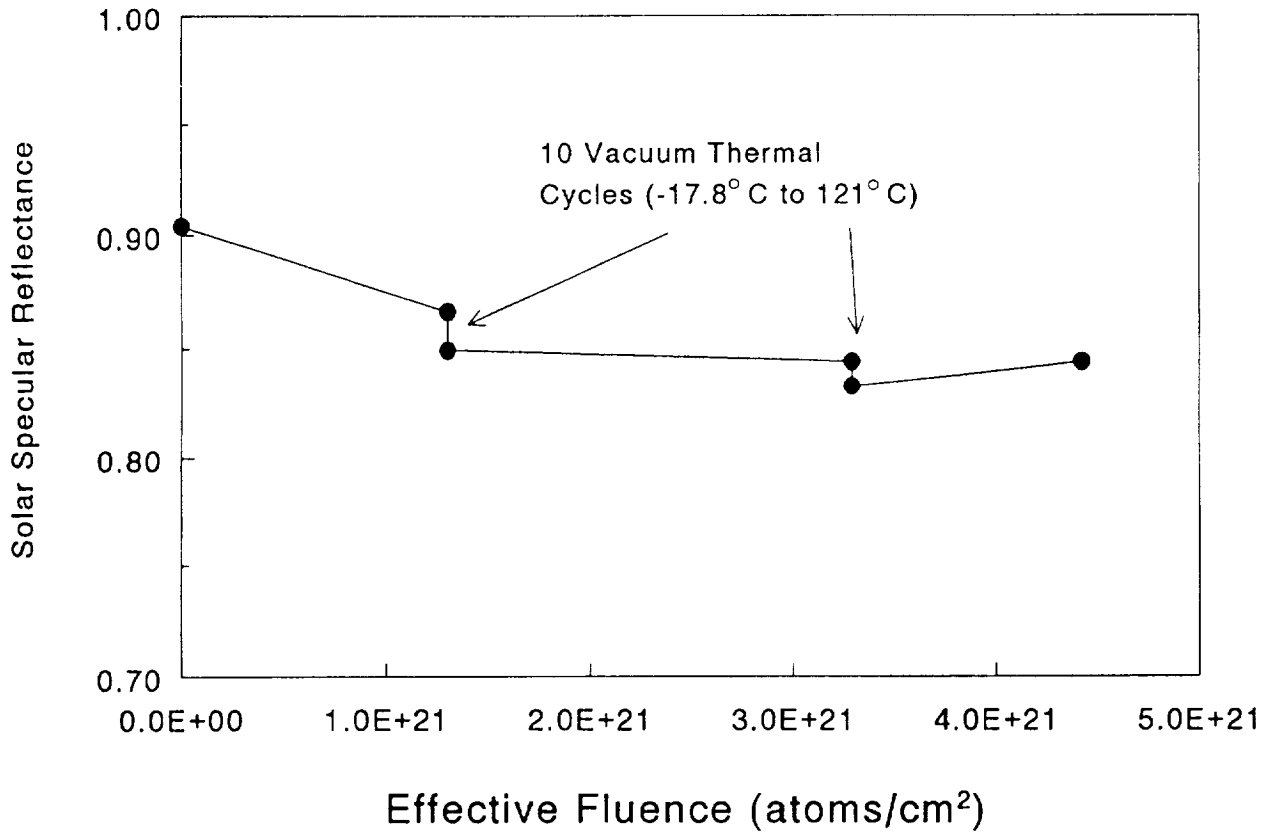


Figure 9: Changes in specular reflectance for solar concentrator coupons exposed to a) 1000 ESH VUV followed by atomic oxygen (effective fluence =  $1.4 \times 10^{21}$  atoms/cm<sup>2</sup>) and b) 908 vacuum thermal cycles combined with 893 ESH VUV followed by atomic oxygen (effective fluence =  $1.4 \times 10^{21}$  atoms/cm<sup>2</sup>).

**a**



**b**

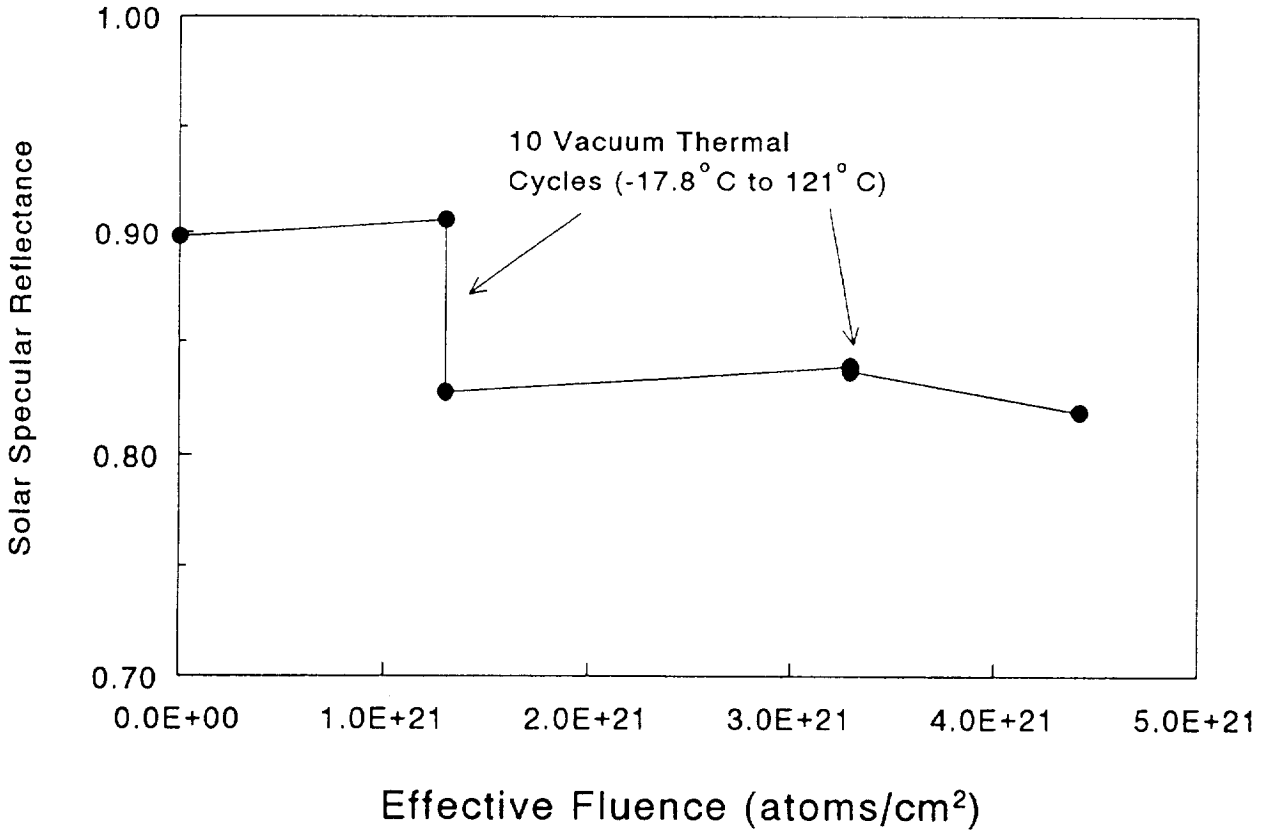


Figure 10: The effect of incremental air plasma ashing and thermal cycling on the solar specular reflectance of sol-gel mirrors for a) Sample A and b) Sample B.